# HEREDITY INTEGRAL DRIFT COMPENSATION IN PIEZORESISTIVE CONTACT STRESS SENSORS

*Otto, J.K., +Brown, T.D., Heiner, A.D., Callaghan, J.J.
*+Department of Orthopaedic Surgery and Biomedical Engineering, University of Iowa, 2181E Westlawn, Iowa City, IA 52242
Phone: (319) 335-7528, Fax: (319) 335-7530, E-mail: tom-brown@uiowa.edu

**Introduction:** Many practical orthopaedic research applications of piezoresistive contact stress sensors involve relatively long-term (multi-minute) load applications. Unfortunately, accumulation of drift artifact often limits contemporary sensor accuracy to much shorter periods (tens of seconds). Long-term drift errors have been documented to be as much as 35% [1] to 50% [2] after 2 hours of static loading. We here introduce a Boltzmann heredity integration algorithm that allows compensation for the great majority of such drift, thus greatly increasing sensor accuracy.

**Methods:** Analogously to the approach used for stress/strain analysis of viscoelastic continua, raw sensor output, $P_{raw}(t)$, can be transformed to drift-compensated sensor output, $P_{bolz}(t)$, using a time-dependent characteristic function, $C(t)$:

$$P_{bolz}(t) = \int_0^t C(t-t)\frac{dP_{raw}(t)}{dt}dt$$

Here, $t$ is a dummy variable of integration. Analogously to a viscoelastic solid, when a step input of constant contact stress, $s_0$, is applied to the sensor, drift effects take the form of a general exponential curve, $P_{raw}(t) = a_0 + a_1(1 - e^{a_2 t})$, where $a_0$, $a_1$, and $a_2$ are empirical constants. In the (Laplace transform) s-domain, $C(s)$ is related to $P_{raw}(s)$ through the expression:

$$C(s) = \frac{s_0}{P_{raw}(s)s^2}$$

Converted back into the time-domain, $C(t)$ becomes the key term for compensating for the effects of drift.

This compensation algorithm was applied to a commercially available multiplexed array sensor (K-Scan, Tekscan Inc., Boston, MA) having 22 columns and 26 rows of conductors, between which a layer of piezoresistive ink was deposited. Each column/row intersection defined a sensing cell (sensel) 1.61 $mm^2$ in area. The thickness of the sensor was 0.10 mm. Testing was performed in a specially designed 152 mm diameter aluminum pressure vessel, consisting of a body and a base (Figure 1). The body housed a hydraulic cylinder, a pressure transducer, and a 0.79 mm thick nitrile membrane which retained hydraulic fluid. The piezoresistive sensor was placed between the membrane and the base, and the two sections were bolted together. The actuator of a Bionix 858 machine supplied transient force to the hydraulic cylinder piston, generating transient hydrostatic pressure within the fluid, and transferring spatially homogenous contact stress through the membrane to the surface of the sensor. The pressure transducer output, $P_{true}(t)$, provided a gold standard for comparison to piezoresistive sensor output.

Several loading histories were chosen representative of actual cadaver or joint prosthesis experiments, with maximum contact stress ($P_{max}$) and loading period as parametric variables (Table 1). Prior to each experiment, the sensor was equilibrated and auto-calibrated using two fiduciary stress levels (20% and 80% of anticipated maximum contact stress). Inter-experimental drift effects were minimized by unloading the sensor for at least twice the duration of the previous test. First, constant static loads were applied to the sensor for a period of 15 minutes (900 sec) at 5, 10, 15, and 20 MPa. General exponential curvefits of the $P_{raw}(t)$ data were generated, and the necessary $C(t)$ functions were computed. To demonstrate the algorithm's ability to deal with arbitrary load waveforms, the sensor was loaded with ramps, steps, and hybrid loads (Figure 2). Compensated sensor output was computed by numerical integration of the Boltzmann integral. The $C(t)$ function obtained from the 10 MPa static case was used to evaluate the non-static cases. To assess the effectiveness of the correction, areas under the $P_{raw}(t)$ and $P_{bolz}(t)$ versus time curves were normalized to the area under the corresponding $P_{true}(t)$ curve (effectively, the local impulse $L$).

**Results & Discussion:** Compared to original sensor output, drift compensation eliminated an average of 83% of the raw signal's error. (The static cases yielded impulse ratios of identically 1.00 because the $C(t)$ functions were generated from these experiments). The non-static cases demonstrated that arbitrary loading histories could be used. In principle, a family of $C(t)$ functions could be used to form a characteristic function that is also stress-dependent, to achieve additional accuracy during drift compensation.

**References:**

[1] Werner, F.W. *et al*. *Trans. 41st ORS*: 705, 1995
[2] Otto, J.K. *et al*. *Trans. 44th ORS*: 808, 1998.

**Acknowledgements:** Financial support was provided by Johnson & Johnson Orthopaedics. Dr. Joan Bechtold's kind cooperation was greatly appreciated.

**Figure 1**

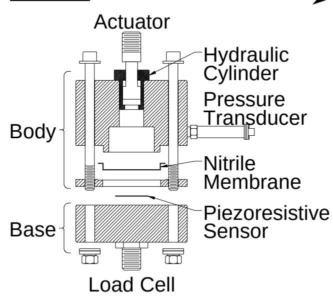


**Table 1**

| $P_{max}$ (MPa) | Loading Type | Period (sec) | $\Lambda_{raw}/\Lambda_{true}$ | $\Lambda_{bolz}/\Lambda_{true}$ |
|---|---|---|---|---|
| 5 | static | 900 | 1.19 | 1.00 |
| 10 | static | 900 | 1.21 | 1.00 |
| 15 | static | 900 | 1.16 | 1.00 |
| 20 | static | 900 | 1.10 | 1.00 |
| 15 | ramp | 100 | 1.08 | 1.06 |
| 15 | ramp | 200 | 1.13 | 1.06 |
| 15 | ramp | 400 | 1.19 | 1.04 |
| 15 | ramp | 800 | 1.27 | 1.04 |
| 15 | step | 600 | 1.17 | 1.00 |
| 15 | hybrid | 600 | 1.19 | 1.01 |

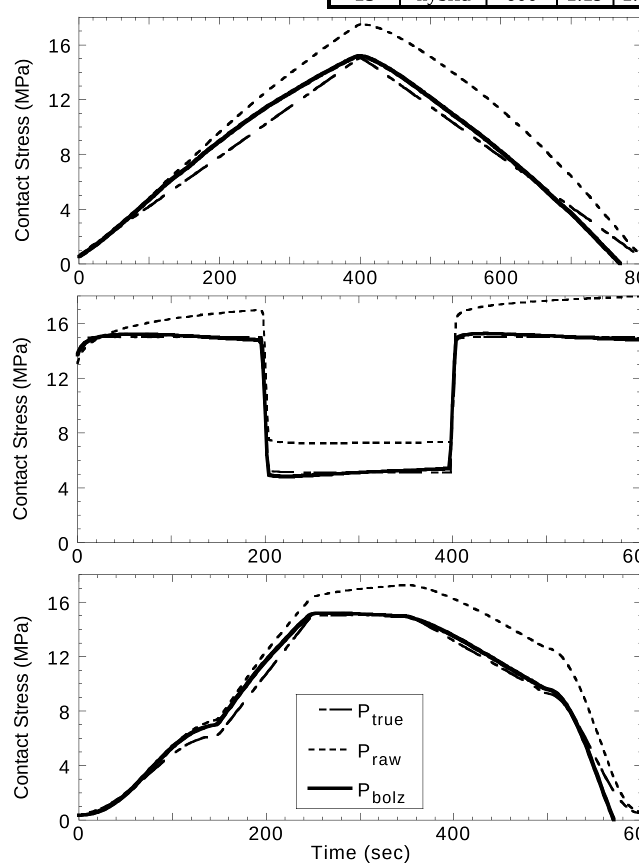


Figure 2. Non-static loading. Top: ramp, Middle: step, Bottom: hybrid.

☒ One or more of the authors have received something of value from a commercial or other party related directly or indirectly to the subject of my presentation.

☐ The authors have not received anything of value from a commercial or other party related directly or indirectly to the subject of my presentation.